

## Conditional damped random surface velocity model of turbulent jet breakup

Ben Trettel

Department of Mechanical Engineering, University of Texas at Austin, Texas  
ben.trettel@gmail.com

### Abstract

A turbulent jet breakup model is derived using concepts from probability theory. Velocity fluctuations at the free surface are hypothesized to be the cause of turbulent jet breakup. We formalize this idea by treating the fluctuations as random variables, subject to damping from the free surface. In contrast to previous theories, we use a conditional ensemble average to determine quantities of interest because not all fluctuations produce droplets. An energy balance and a closure model are used to determine the Sauter mean diameter. Similar approaches are used to determine the breakup onset location, breakup length, and spray angle. A criteria for the transition to the turbulent atomization regime is derived under the hypothesis that the cause is a change in the minimum velocity from the Hinze scale to the Kolmogorov scale. To validate the model, we compiled data from previous experimental studies using long pipe nozzles. The little data for rough pipes was used to include turbulence intensity in our study.

Keywords: turbulent breakup, turbulence intensity, Reynolds number, integral scale, nozzle geometry effects, droplet size, SMD, droplet velocity, breakup regimes, breakup length, breakup onset location, spray angle

### Introduction

It is well known that liquid jet turbulence influences jet breakup, but the details are unclear. We identify four separate turbulent jet breakup effects: 1. *hydrodynamic* regime effects (turbulent vs. laminar, separate from *breakup* regimes); 2. Reynolds number effects; 3. turbulence intensity effects (the “level of turbulence”); and 4. turbulence scale or spectrum effects (integral scale,  $\Lambda$ , or energy spectrum,  $E(\kappa)$ ). We develop a turbulent jet breakup model, the conditional damped random surface velocity (CDRSV) model, which considers effects 2 through 4, for the most basic breakup quantities. We focus on circular non-cavitating turbulent Newtonian liquid jets ejected into quiescent gases with a liquid to gas density ratio  $\rho_l/\rho_g \gtrsim 500$  so that aerodynamic effects are negligible [1]. The model is comparable or superior to previous analytical models, though ultimately the accuracy is insufficient for applications. Better estimates can be found from regressions developed from the large experimental database we compiled.

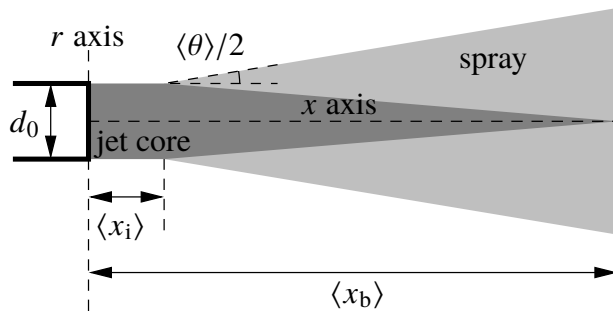
### Dependent quantities of interest and nomenclature

Figure 1 shows a slice through the center of a statistically steady ensemble averaged circular liquid jet ejected from left to right into a quiescent gas. The nozzle exit plane is denoted with 0, e.g., the nozzle orifice diameter is  $d_0$ . The  $x$  axis starts at the center of the nozzle exit plane and is oriented with the jet’s velocity ( $\bar{U}_0$ ). The  $r$  axis extends radially from the center. The quantities of interest (QoIs) are the average droplet diameter at formation ( $D_{ij}$ ; e.g.,  $D_{32}$  for the Sauter mean diameter), average droplet radial velocity at formation ( $\langle v_d \rangle$ ), average breakup length ( $\langle x_b \rangle$ ), average breakup onset location ( $\langle x_i \rangle$ ), and average (full) spray angle ( $\langle \theta \rangle$ ). See Lefebvre and McDonell [2] for the precise definitions of the QoIs. We drop the phrase “average” for the QoIs from here. Bars denote spatial averages, and angle brackets denote ensemble averages. In this work the Reynolds number is  $Re_{ij} \equiv \bar{U}_j d_j / \nu_i$  for location  $j$  (0 for nozzle exit) and fluid  $i$  (l for liquid, g for gas). The Weber number is  $We_{ij} \equiv \rho_i \bar{U}_j^2 d_j / \sigma$ .  $u' \equiv \langle U - \langle U \rangle \rangle^{1/2}$  and  $v' \equiv \langle V - \langle V \rangle \rangle^{1/2}$  are the RMS velocities in  $x$  and  $r$ .  $k \equiv (u'^2 + v'^2 + w'^2)/2$  is the turbulent kinetic energy.  $\Lambda$  is the integral length scale. To simplify the results, the spatially averaged *isotropic* ( $u' = v' = w'$ ) RMS velocity is defined as  $\bar{u}' \equiv (2\bar{k}_j/3)^{1/2}$ , not averaging over  $u'_j$  directly. This allows  $\bar{Tu}_j^2 \equiv (\bar{u}'_j/\bar{U}_j)^2 \equiv 2\bar{k}_j/(3\bar{U}_j^2)$ .

### Previous quantitative theories of turbulent jet breakup

Only theories with explicit  $Tu$  or  $k$  dependence are considered. Table 1 summarizes the QoIs in each study.

Natanzon [3] developed the earliest quantitative theory of turbulent jet breakup we are aware of. Natanzon applied the maximum entropy principle with a kinetic energy constraint using  $k$  to find the droplet diameter distribution and that  $D_{30} \approx 8.454\sigma/(\bar{k}_0\rho_l)$ . Sitkei [4] and Lebedev [8] use a simpler energy balance, obtaining the same scaling. Wu et al. [9] use similar arguments combined with inertial range scaling to estimate  $D_{32}$ . Broadly, these arguments have three problems: 1. the arguments implicitly assume that the droplets have zero velocity at



**Figure 1.** Variables labeled on a schematic liquid jet.

	$D_{ij}$	$\langle v_d \rangle$	regime	$\langle x_i \rangle$	$\langle x_b \rangle$	$\langle \theta \rangle$
Natanzon [3]	•	•		○	○	•
Sitkei [4]	•	○				•
Skrebkov [5]	•	•	•			•
Tsyapko [6, 7]				○	•	•
Lebedev [8]	•					
Wu et al. [9–11]	•	○	○	•	•	
Huh et al. [12]	•	○				•
Kerstein et al. [13]	•			•		
This work	•	•	•	•	•	•

**Table 1.** QoIs in many turbulent breakup theories. •, explicit; ○, implicit

formation because all input energy (e.g., turbulent kinetic energy) is used to create new free surface; 2. the arguments assume that replacing all quantities with their averages (or a “representative” value) is mathematically valid, but this is often false (e.g., the RANS closure problem); and 3. aside from Natanzon, the theories do not justify which characteristic diameter ( $D_{ij}$ ) is appropriate. In contrast, Skrebkov [5] and Huh et al. [12] assume that a representative droplet diameter equals the integral scale  $\Lambda$  multiplied by a constant, avoiding problem 1 but not the others. However, as the integral scale is the largest turbulent scale, this seems plausible for only the largest droplet diameter.

The experiments of Wu et al. [9, p. 305] suggest that  $\langle v_d \rangle$  may scale with the radial turbulent RMS velocity  $v'$ . Tsyapko [7] and Huh et al. [12] developed spray angle  $\langle \theta \rangle$  models with this assumption. Rather than assuming this scaling, Skrebkov [5] used a energy balance including  $v'$  to determine  $\langle v_d \rangle$  and  $\langle \theta \rangle$ . We use a force balance.

Wu et al. [9] and Kerstein et al. [13] estimate the breakup onset location  $\langle x_i \rangle$  by finding the time required for breakup to occur, but they estimate this time differently. Kerstein et al. is more consistent with the data aside from the proposed  $Re_{10}$  dependence. Our model replaces the  $Re_{10}$  dependence with a  $\overline{Tu}_0$  dependence.

Natanzon [3, p. 5R] assumed all breakup occurs at the nozzle exit, so  $\langle x_b \rangle = 0$ . Wu and Faeth [10, p. 2916R] assumed the jet core ends where the local droplet diameter increases to the local jet diameter. Neither approach directly predicts where the jet core ends. In contrast, Tsyapko [6, p. 13] used a jet geometry model to relate  $\langle x_b \rangle$  to  $\langle \theta \rangle$ . We take a direct approach by estimating the surface mass flux to find where the jet core erodes completely.

### Experimental data compilation

We compiled an experimental database for all QoIs for model validation. The database is limited to non-cavitating liquid jets ejected from long pipes (“pipe jets”) at low Mach numbers ( $< 0.4$ ). Excluding non-pipe jets reduces the impact of factors which are typically unknown but roughly constant for fully developed (“FD”) pipes, e.g., the velocity profile and  $\Lambda_0$ . Using solely pipe nozzles also allows us to estimate  $\overline{Tu}_0$ . Frequently, the turbulence intensity is assumed to be roughly constant or a function of only the Reynolds number, making it unnecessary in models. The Reynolds number is often seen as a measure of “how turbulent” a flow is, but this is mistaken. In FD smooth pipe flow,  $\overline{Tu}$  *decreases* as  $Re_{10}$  increases [14, p. 6], contrary to what most expect. Nozzles do not necessarily have monotonically increasing or decreasing trends [8, figs. 2–4]. For a particular nozzle, the outlet turbulence intensity  $\overline{Tu}_0$  is a function of  $Re_{10}$  and the nozzle inlet  $\overline{Tu}$ . Different nozzles have different trends, so both variables are needed.

To estimate  $\overline{Tu}_0$ , we developed a regression between the friction factor and  $\overline{Tu}_0$  ( $\equiv (2\overline{k}_0/3)^{1/2}/\overline{U}_0$ ) for FD pipe flows [14]:  $\overline{Tu}_0 = 0.3655f^{0.4587}$  (9 smooth and 8 rough points,  $R^2 = 0.9753$ ). As  $\overline{Tu}_0$  in smooth FD pipe flows is a function of only  $Re_{10}$ , rough pipes are needed to avoid confounding between  $Re_{10}$  and  $\overline{Tu}_0$ . Unfortunately we are aware of only three rough pipe jet breakup studies. Skrebkov [5] has 3 measurements of  $\langle \theta \rangle$ , Kusui [15] has over 150 measurements of  $\langle x_b \rangle$ , and Kim [16] has 2 photographs which can be analyzed to estimate  $\langle x_i \rangle$ . Kusui had a  $8.75d_0$  smooth section after their rough pipe, complicating estimating  $\overline{Tu}_0$ . Presumably  $\overline{Tu}$  decays in the smooth section. However, a power law regression of pipe data for  $\langle x_b \rangle$  fits non-pipe data [17, 18] best with no decay. While we assume there is no decay in  $\overline{Tu}_0$  in this work, ultimately, Kusui’s data is imprecise about how  $\langle x_b \rangle$  varies with  $\overline{Tu}_0$ .

## Theory and discussion

### Turbulence evolution in liquid jets

Understanding how turbulence quantities ( $k$  and  $\Lambda$ ) evolve spatially in the jet is required to develop models of the breakup of the entire jet. Kim [16, p. 23] and Huh et al. [12, p. 458] used turbulence models to estimate the decay of turbulence in the jet. Experiments show that turbulence in a liquid jet decays at the centerline initially [19, p. 3390].

However, shear at the jet surface causes production of turbulence, such that  $k$  can increase. As droplets are formed at the free surface, using solely decay is not necessarily correct if production is significant. The measurements of Mansour and Chigier [19, p. 3389] suggest that  $k$  at the jet boundary grows slowly downstream. This is inconsistent with the measurements of Wolf et al. [20, p. 402L], which suggest that  $k$  only decays. Given the complexity of turbulence modeling, we will use the approximation of Wu et al. [9, p. 308]:  $k$  and  $\Lambda$  do not vary downstream. The turbulence will also be approximated as homogeneous in the radial and angular directions and isotropic. Spatial averaged  $\bar{k}$  will approximate the  $k$  profile. In reality,  $k$  peaks near the free surface, becoming more homogeneous downstream. Better models considering the inhomogeneity and anisotropy will be the subject of future work.

### **Droplet radial velocity $v_d$ for a particular eddy and the Hinze scales — the conditioning and damping**

A model of the droplet formation process is needed. Consider a random turbulent velocity fluctuation  $v$  (mean zero) at the free surface at time 0 (so  $\tilde{v}(t=0) = v$ ). A droplet forms if the radial velocity  $\tilde{v}(t) > 0$  when a droplet detachment condition is met. Surface tension opposes/damps the turbulent fluctuations. This force  $F_\sigma = A \cdot p_\sigma$  where  $A$  is the cross-sectional area of the surface perturbation and  $p_\sigma = 2\sigma/R$  is the capillary pressure, where  $R$  is the radius of curvature. We assume that the surface perturbations are spherical, with a radius of curvature  $R$  equal to the distance  $\delta$  the eddy penetrates outside the free surface (see figure 2). Multiplying by an arbitrary constant, we find that  $F_\sigma = 2\pi C_F \sigma \delta$ . We assume that the eddy has a diameter proportional to  $\ell \equiv 2\pi/\kappa$ , where  $\kappa$  is the wavenumber of the turbulence associated with the velocity fluctuation  $v$ . (Note that despite the eddy's nominal diameter being  $\ell$ , we select the radius of curvature as  $\delta$  for simplicity.) The eddy's mass then is  $C_V \rho_l \pi \ell^3 / 6$ , with another arbitrary constant. The equations of motion of the eddy as it penetrates the surface are

$$\frac{d\delta}{dt} = \tilde{v} \quad \text{and} \quad -2\pi C_F \sigma \delta = C_V \rho_l \frac{\pi}{6} \ell^3 \frac{d\tilde{v}}{dt}, \quad (1)$$

which have the solutions

$$\delta = v t_R \sin\left(\frac{t}{t_R}\right), \quad \tilde{v} = v \cos\left(\frac{t}{t_R}\right), \quad \text{where} \quad t_R^2 \equiv \frac{C_V \rho_l \ell^3}{12 C_F \sigma}. \quad (2)$$

If we assume that the droplet detaches after traveling a distance  $\delta = C_{\text{lig}} \ell$  ( $C_{\text{lig}} \gtrsim 2$ , so that detachment occurs when the lower end of the ligament is beyond the original free surface location), then we can determine the breakup time  $t_b$  and the droplet velocity at detachment ( $v_d = \tilde{v}(t = t_b)$ ):

$$\frac{t_b}{t_R} = \sin^{-1}\left(\frac{C_{\text{lig}} \ell}{v t_R}\right) \quad \text{and} \quad \frac{v_d}{v} = \sqrt{1 - \frac{12 C_{\text{lig}}^2 C_F \sigma}{C_V \rho_l v^2 \ell}} = \sqrt{1 - \frac{\text{We}_{T,\text{crit}}}{\text{We}_T}}. \quad (3)$$

This model is oversimplified, but it has the desired features. The last term is an inverse eddy Weber number,  $\text{We}_T \equiv \rho_l v^2 \ell / \sigma$ . Droplet formation ( $v_d > 0$ ) requires that  $\text{We}_T > \text{We}_{T,\text{crit}} \equiv 12 C_{\text{lig}}^2 C_F / C_V$ . As such, minimum scales for droplet formation exist. An arbitrary eddy velocity  $v$  can be related to a corresponding eddy wavenumber  $\kappa$  with  $v = \sqrt{\kappa E(\kappa)}$  [21, p. 222]. If we assume that the minimum scales are in the inertial range and apply  $v = \sqrt{\kappa E(\kappa)}$  to the inertial range spectrum  $E(\kappa) = C_K \varepsilon^{2/3} \kappa^{-5/3}$  ( $C_K = 1.5$  [22, p. 231]), we find that  $\ell = 2\pi v^3 / (C_K^{1/2} \varepsilon)$ . From there we can calculate the Hinze scales [23, 24], the smallest for which droplet formation can occur ( $v_d = 0$ ):

$$v_\sigma \equiv \underbrace{\left(\frac{\text{We}_{T,\text{crit}}}{2\pi}\right)^{1/5}}_{C_{v_\sigma}} \left(\frac{\sigma \varepsilon}{\rho_l}\right)^{1/5} \quad \text{and} \quad \ell_\sigma \equiv \underbrace{\left(\frac{2\pi C_{v_\sigma}^3}{C_K^{1/2}}\right)^{1/5}}_{C_{\ell_\sigma}} \left(\frac{\sigma^3}{\rho_l^3 \varepsilon^2}\right)^{1/5}. \quad (4)$$

The velocity  $v_\sigma$  is the minimum for droplets to form *if surface tension dominates*. At high Weber numbers  $v_\sigma$  may decrease below  $v_K$ , the Kolmogorov velocity scale, and in that case  $v_K$  will be the minimum. We use the term  $v_{\text{min}}$  for whichever minimum applies. Because not all fluctuations produce droplets, the ensemble averages we calculate will be conditioned on droplet formation, abbreviated DF. The condition notation will be dropped for terms which imply breakup occurs, e.g.,  $\langle v_d \mid \text{DF} \rangle$  would be redundant. Additionally, we'll use  $v_{\text{min}} = v_\sigma$  for simplicity unless otherwise noted in this paper. Analogous expressions for  $v_{\text{min}} = v_K$  are easily found.

We are unaware of data capable of validating the minimum droplet velocity and diameter estimates. The smallest droplet observed by Wu [25, p. 36] was  $3 \mu\text{m}$  in diameter ( $< 0.5 \mu\text{m}$  uncertainty,  $\rho_l/\rho_g < 40$  so aerodynamic effects are present), but insufficient detail was provided to estimate  $\ell_\sigma$  or  $\ell_K$  for this case. The smallest droplets measured by Wu et al. [9, p. 307] ( $\rho_l/\rho_g > 500$ ) were said to be much larger than  $\ell_K$  in the second wind-induced regime. The DNS study of McCaslin and Desjardins [26, p. 5, fig. 2b] suggests that surface perturbations are suppressed for scales smaller than  $\ell_\sigma$  if  $\ell_\sigma > \ell_K$ . We hypothesize that droplet diameter scales with surface perturbation size.

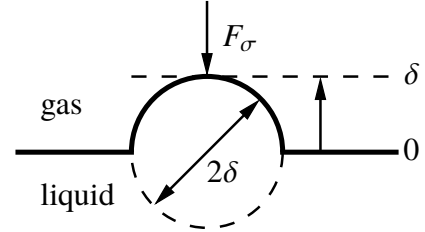


**Figure 2.** Eddy penetrating surface.

**Average droplet diameter  $D_{32}$  and average droplet radial velocity  $\langle v_d \rangle$** 

Wu et al. [9, p. 312] assume that  $D_{32}$  scales with a representative length (in our terminology,  $D_{32} \propto \langle \ell \mid \text{DF} \rangle$ ), however, we will not assume this.  $D_{32}$  is controlled by the surface energy, not the size of the eddies directly. Energy conservation suggests (assuming the process is adiabatic and neglecting rotational and other energies):

$$\frac{1}{2}\rho_1\mathcal{V}\left[\left(\bar{U}_0 + u\right)^2 + v^2 + w^2\right] = \sigma SA + \frac{1}{2}\rho_1\mathcal{V}\left(u_d^2 + v_d^2 + w_d^2\right), \quad \text{or simplified: } \sigma\frac{SA}{\mathcal{V}} = \frac{1}{2}\rho_1\left(v^2 - v_d^2\right), \quad (5)$$

where in the first equation the left side is before breakup and the right side is after breakup. We assumed that only one droplet is formed per eddy event. The eddy/droplet has volume  $\mathcal{V}$ , and the formed droplet has surface area  $SA$ . The model also implicitly assumes that  $v_d$  and droplet diameter  $D$  are perfectly correlated. For simplicity we assume that the  $r$  direction is always normal to the liquid surface, accurate for large  $\langle x_b \rangle/d_0$ . Like  $v$  ( $= \bar{v}(t=0)$  as before),  $u$  and  $w$  are turbulent velocity fluctuations with mean zero defined in the streamwise and angular directions, respectively. The mean velocities in the radial and angular directions are zero. (If the jet is decelerating, there is a mean  $\bar{V}$  as well, however, we neglect this as we assume aerodynamic drag is negligible.) We assume that the free surface does not affect streamwise or angular velocities such that  $u_d \equiv \bar{U}_0 + u$  and  $w_d \equiv w$ . These cancel, leaving the surface area to volume ratio to be determined by the energy left over from the damping. Now, we apply the conditional average and the model for  $v_d$  (equation 3), and note that by hypothesis  $\langle SA/\mathcal{V} \rangle \approx \langle SA \rangle / \langle \mathcal{V} \rangle = 6/D_{32}$ :

$$\sigma\left\langle\frac{SA}{\mathcal{V}}\right\rangle = \frac{1}{2}\rho_1\left\langle v^2 - v_d^2 \mid \text{DF} \right\rangle = \frac{1}{2}\rho_1\text{We}_{\text{T,crit}}\left\langle\frac{v^2}{\text{We}_{\text{T}}}\right\rangle, \quad \text{which returns } D_{32} = \frac{12}{\text{We}_{\text{T,crit}}}\left\langle\ell^{-1} \mid \text{DF}\right\rangle^{-1} \quad (6)$$

Contrary to Wu et al.'s assumption,  $D_{32}$  is proportional to the *harmonic mean*  $\langle \ell^{-1} \mid \text{DF} \rangle^{-1}$ , not the *arithmetic mean*  $\langle \ell \mid \text{DF} \rangle$ . The two terms are the same to first-order, but not identical. This term is unclosed, so it requires a model.

The concept of an ‘‘eddy’’ in this work will be clarified. The length  $\ell$  associated with a particular velocity fluctuation  $v$  is ambiguous. The energy spectrum as used by Wu and Faeth [10, p. 2916] can relate  $v$  and  $\ell$ , but this is only a heuristic. More than one ‘‘eddy’’ can contribute to velocity fluctuations at a particular location. Smaller lengths likely have only one eddy contribution, making the idea behind the Hinze scales reasonable. Larger velocity fluctuations may involve more than one eddy, making the spectrum heuristic incorrect. We’ll use the functional form of the average to inform the choice of the model. For  $D_{32}$  specifically, we’ll use the inertial range spectrum, as the average is more strongly influenced by the smallest scales. Averages controlled by larger scales require a different length scale specification. The inertial range spectrum with the dissipation model  $\bar{\varepsilon}_0 = C_\varepsilon \bar{k}_0^{3/2} / \Lambda_0$  (we choose  $C_\varepsilon = 0.43$  [22, p. 244]) suggests  $D_{32} \propto \langle v^{-3} \mid \text{DF} \rangle$ , which can be computed with a prescribed PDF.

To maintain analytical tractability, a power law velocity PDF ( $f_v(v) = C v^{-\alpha}$ ) will be used. A Gaussian PDF would be more realistic, but will be used in future work to keep this work simple. Generally  $\langle v^\beta \mid v > v_{\min} \rangle \propto \bar{v}^{\beta} f(v_{\min}/\bar{v})$  (implying  $\langle v_d \rangle \propto \bar{v}'$  as hypothesized by Wu et al. [9, p. 305]), but for power law PDFs  $\langle v^\beta \mid v > v_{\min} \rangle \propto v_{\min}^\beta$  with no  $\bar{v}'$  dependence. (Again, DF means  $v > v_{\min}$  here.) Using a power law PDF, we find that  $\langle v^{-3} \mid v > v_{\min} \rangle = (\alpha - 1)v_{\min}^{-3}/(\alpha - 2)$ . To compute  $D_{32}$ , we start with equation 6, then use the inertial range spectrum to eliminate  $\ell$ , substitute in the dissipation and  $\langle v^{-3} \mid v > v_{\min} \rangle$  models, and choose  $v_{\min} = v_\sigma$  (equation 4) to find

$$\frac{D_{32}}{d_0} = \frac{24\pi}{\text{We}_{\text{T,crit}}}\frac{\langle v^{-3} \mid v > v_{\min} \rangle}{C_{\text{K}}^{1/2}\varepsilon} = \frac{24\pi}{\text{We}_{\text{T,crit}}}\frac{\alpha - 2}{\alpha - 1}\left(\frac{v_\sigma}{v'_0}\right)^3\frac{\Lambda_0}{d_0} = C_{D_{32}}\bar{\text{Tu}}_0^{-6/5}\text{We}_{10}^{-3/5}\left(\frac{\Lambda_0}{d_0}\right)^{2/5}. \quad (7)$$

which has a similar scaling to Wu et al. [9, p. 308] for the initial value of  $D_{32}$ , despite the difference in the definition. This is a consequence of the power law PDF. Alternative choices could make how  $\langle \ell \mid \text{DF} \rangle$  and  $\langle \ell^{-1} \mid \text{DF} \rangle^{-1}$  scale differ. To find the average droplet velocity  $\langle v_d \rangle$  we start with equation 3 and apply an approach similar to that for  $D_{32}$ , noting that  $\langle v^{-5} \mid v > v_{\min} \rangle = (\alpha - 1)v_{\min}^{-5}/(\alpha + 4)$  for a power law PDF. We find that

$$\frac{\langle v_d \rangle}{v'_0} \approx \frac{\langle v \mid \text{DF} \rangle}{v'_0}\left(1 - \text{We}_{\text{T,crit}}\frac{\sigma}{\rho_1 v^2 \ell} \mid \text{DF}\right)^{1/2} = \frac{v_{\min}}{v'_0}\left(\frac{\alpha - 1}{\alpha - 2}\right)\left(1 - C_{\text{K}}^{1/2}\frac{\alpha - 1}{\alpha + 4}\right)^{1/2} = C_{v_d}\bar{\text{Tu}}_0^{-2/5}\left(\text{We}_{10}\frac{\Lambda_0}{d_0}\right)^{-1/5}. \quad (8)$$

The theory will now be compared against experimental data. Only initial droplet diameter and velocity measurements are compared because the constant  $k$  and  $\Lambda$  approximations may be inaccurate downstream. For initial  $D_{32}$ , three data sources are available [1, 9, 27]. For initial droplet radial velocity, the only available data is from Wu

et al. [9, p. 305]. None of these sources have rough tubes, so the data has almost no variation in  $\overline{Tu}_0$ . Because of confounding between  $\overline{Tu}_0$  and  $Re_{10}$  we used solely the variable  $\overline{Tu}_0^2 We_{10}$  in the regression analysis, consistent with the theory. The fitted power law equations are ( $D_{32}$ : 29 points,  $R^2 = 0.8204$ ;  $\langle v_d \rangle$ : 17 points,  $R^2 = 0.0304$ ):

$$\frac{D_{32}}{d_0} = 0.8082 \left( \overline{Tu}_0^2 We_{10} \right)^{-0.6988}, \quad \text{and} \quad \frac{\langle v_d \rangle}{v'_0} = 0.0487 \left( \overline{Tu}_0^2 We_{10} \right)^{0.0607}. \quad (9)$$

The regressions apply for the second wind-induced regime with  $6.5 \cdot 10^4 < Re_{10} < 1.0 \cdot 10^6$ ,  $4.7\% < \overline{Tu}_0 < 6.1\%$ , and  $2.3 \cdot 10^4 < We_{10} < 1.9 \cdot 10^6$ . For  $D_{32}$ ,  $5.9 \cdot 10^2 < \rho_l/\rho_g < 6.2 \cdot 10^3$ . For  $\langle v_d \rangle$ ,  $5.9 \cdot 10^2 < \rho_l/\rho_g < 9.6 \cdot 10^3$ . The coefficient of the  $D_{32}$  theory is near that found in the regression. The measurement error in  $\langle v_d \rangle$  is large, making a close fit impossible for both the regression and theory. Given the small variation in  $\overline{Tu}_0$  for the data, for the moment the most that can be said is that the theory is not inconsistent with the data.

### Transition from the second wind-induced regime to the atomization regime

A popular atomization regime criteria is  $We_{g0} > 40.3$ , introduced by Miesse [34, p. 1697]. Reitz [35, pp. 4–9] notes that water jet cutting jets are more stable than existing criteria suggest. Presumably this is due to  $\overline{Tu}_0$  not being considered, as  $\overline{Tu}_0$  is lower in cutting jets than diesel sprays. We consider atomization due to turbulence only, with no aerodynamic or cavitation influence. The  $We_{g0}$  criteria is based on aerodynamic atomization. When using breakup length to objectively determine regime (contrast with subjective visual methods), a change in the trend from a power law (second wind-induced regime) to a plateau (or otherwise) marks the onset of atomization. Using that definition, Kusui [15, p. 1067] proposed an empirical criteria which uses the friction factor of rough pipe nozzles. Kusui's  $\overline{Tu}_0$  is unclear, but we assume that  $\overline{Tu}_0 \propto f^{0.4587}$ . Rearranging Kusui's equation and exponentiating so that  $We_{10}$  has a power of 1, Kusui's classifying variable is  $TA_{Kusui} \equiv \overline{Tu}_0^{0.32} We_{10} Re_{10}^{-0.94} (\nu_l/\nu_g)^{-0.67}$ , where  $TA_{Kusui} > TA_{crit,Kusui}$  for atomization. Kusui's raw regime data can not be extracted due to ambiguities in the plot, however, we can compare Kusui's variable to our theory. Neglecting aerodynamic effects and cavitation, as the Weber number increases the only discontinuous change is that the minimum velocity scale ( $v_{min}$ ) switches from the Hinze scale ( $v_\sigma$ ) to the Kolmogorov scale ( $v_K \equiv C_{vK} (\varepsilon \nu)^{1/4}$ ). We hypothesize this change corresponds to the onset of the turbulent atomization regime. This is consistent with the lack of  $Re_{10}$  dependence for QoIs in the second wind-induced regime, as the Hinze scale does not contain viscosity. Equating  $v_\sigma$  and  $v_K$  and rearranging defines the critical turbulent atomization number:

$$TA_{crit} \equiv \left( \frac{C_{v\sigma}}{C_{vK}} \right)^5 \equiv \left[ \frac{\rho_l \varepsilon^{1/4} \nu_l^{5/4}}{\sigma} \right]_{crit} = C_\varepsilon^{1/4} \left( \frac{3}{2} \right)^{3/8} \left[ \left( \frac{\overline{Tu}_0^3 d_0}{\Lambda_0} \right)^{1/4} We_{10} Re_{10}^{-5/4} \right]_{crit}. \quad (10)$$

As before  $TA > TA_{crit}$  for atomization. For simplicity we'll define  $\widehat{TA} \equiv \overline{Tu}_0^{3/4} We_{10} Re_{10}^{-5/4}$ . The tasks now are to determine  $\widehat{TA}_{crit}$  and evaluate how well it discriminates the regimes. The signs of all exponents in our theory match those of Kusui. Comparison with regime data from our database (figure 3) is less promising. We determined that  $\widehat{TA}_{crit} = 0.005709$  by taking the  $\rho_l/\rho_g > 500$  data and selecting  $\widehat{TA}_{crit}$  such that half the points we classified as in transition between the second wind-induced and atomization regimes were on each side. We omitted Kusui's rough measurements due to suspected inaccuracy in  $\overline{Tu}_0$ . The criteria appears to work aside from Kusui's smooth experiments, which transition earlier than others'. Neglecting all of Kusui's data, we find that  $\widehat{TA}_{crit} = 0.01022$ , however, we can not justify this omission aside from the inconsistency of Kusui's data.

The theory may still be valid even if Kusui's measurements are accurate. Sallam [11, pp. 87–90] suggested that aerodynamic effects can explain the regime transition even when  $\rho_l/\rho_g \gtrsim 500$ , as turbulence can distort the jet core

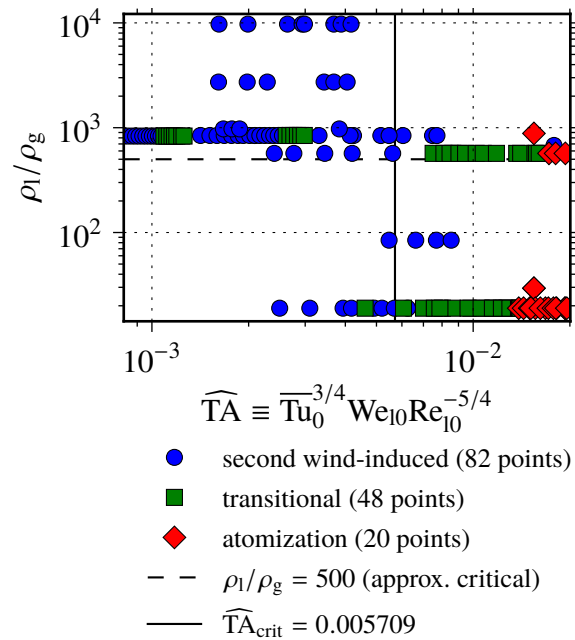


**Figure 3.** Turbulent breakup regime map with experimental data from the database [15, 25, 28–33].

in ways not considered by our theory. The distorted core can then break up due to aerodynamic effects [36]. Phinney [30, pp. 998R–999L] argues that turbulent aerodynamic effects apply when  $\overline{Tu}_0(\rho_1/\rho_g)^{1/2} < 1$ . This estimate is consistent with Wu and Faeth [1]’s  $(\rho_1/\rho_g)_{\text{crit}} = 500$  as the turbulence intensity of that set of experiments at about 5%, leading to  $[\overline{Tu}_0(\rho_1/\rho_g)^{1/2}]_{\text{crit}} \approx 0.05 \cdot \sqrt{500} \approx 1.1$ . Figure 3 contains only smooth pipe data, so there is little  $\overline{Tu}_0$  variation. Consequently, Phinney’s criteria can not explain the failures of the regime boundary, as the criteria is ordered roughly like  $\rho_1/\rho_g$  for this data set, and that line alone discriminates the regimes worse than our theory. A CDRSV model considering the atmosphere could justify a better criteria, and this will be the subject of future work. Tentatively, we speculate that our current boundary may apply only for non-cavitating jets with  $\rho_1/\rho_g \gg 500$ .

### Breakup onset location $\langle x_i \rangle$

We define the breakup onset location as the average distance eddies travel in the time it takes for breakup to occur:  $\langle x_i \rangle \equiv \langle (\overline{U}_0 + \bar{u})t_b \mid \text{DF} \rangle \approx \overline{U}_0 \langle t_b \rangle$  assuming that  $\langle uv \rangle$  is small. To second-order  $t_b = C_{\text{lig}}\ell/\nu$  (see equation 3) so  $\langle t_b \rangle \propto \langle \ell/\nu \mid \text{DF} \rangle$ , which is difficult to model. The term is not influenced by the smallest scales as much as  $D_{32}$ . As such, we assume that the conditioning has little effect. By hypothesis, the parameters influencing the breakup time are  $\sigma$  (N/m),  $\rho_1$  (kg/m<sup>3</sup>), and  $\bar{v}'_0$  (m/s), from which a unique time scale can be formed:  $\langle t_b \rangle \propto \sigma/(\rho_1\bar{v}'_0{}^3)$ , leading to

$$\frac{\langle x_i \rangle}{d_0} = \frac{\overline{U}_0 \langle t_b \rangle}{d_0} = \frac{C_{\text{lig}}\overline{U}_0}{d_0} \left\langle \frac{\ell}{\nu} \mid \text{DF} \right\rangle = C_{x_i} \frac{\overline{U}_0 \sigma}{d_0 \rho_1 \bar{v}'_0{}^3} = C_{x_i} \left( \frac{\overline{U}_0}{\bar{v}'_0} \right)^3 \frac{\sigma}{d_0 \rho_1 \overline{U}_0^2} = C_{x_i} \overline{Tu}_0^{-3} \text{We}_{10}^{-1}. \quad (11)$$

This result is equivalent that of Kerstein et al. [13] if one replaces their  $u_\tau$  with  $\bar{v}'_0$ . Their model would have no  $\text{Re}_{10}$  dependence with this modification. The  $\bar{v}'_0 \propto u_\tau$  scaling implies  $\overline{Tu}_0 \propto \sqrt{f}$ , similar to our correlation for FD pipe flows [14] ( $\overline{Tu}_0 \propto f^{0.4587}$ ). This scaling is consistent with multiple physical pictures, not just the boundary layer scaling described by Kerstein et al. We developed a power law regression of the experimental data [1, 10, 11, 16] (55 points,  $R^2 = 0.6866$ , including  $\rho_1/\rho_g < 500$  data) for  $8.8 \cdot 10^3 < \text{Re}_{10} < 1.0 \cdot 10^6$ ,  $4.7\% < \overline{Tu}_0 < 9.6\%$ ,  $5.1 \cdot 10^3 < \text{We}_{10} < 1.9 \cdot 10^6$ , and  $1.0 \cdot 10^2 < \rho_1/\rho_g < 1.3 \cdot 10^4$ . Due to the confounding of  $\text{Re}_{10}$  and  $\overline{Tu}_0$  from the little data with rough tubes (2 rough points), the Reynolds number was excluded from the regression, which is:

$$\frac{\langle x_i \rangle}{d_0} = 16.0298 \left( \overline{Tu}_0^3 \text{We}_{10} \right)^{-0.9567}. \quad (12)$$

The exponent of the regression is near that of the theory. While the data was in the second wind-induced regime, the theory is independent of the minimum scale, and therefore the regression and theory may also apply for atomization.

### Breakup length $\langle x_b \rangle$

To determine the breakup length, we first calculate the average surface mass flux from the jet,  $\langle \dot{m}'' \rangle$ . We decompose the surface into waves of wavenumbers  $\kappa \propto 1/\ell$  in the streamwise and angular directions. We assume droplets are formed with frequency  $\nu/\ell$  and mass proportional to  $\rho_1 \ell^3$ . We ensemble average to determine  $\langle \dot{m}'' \rangle$ :

$$\langle \dot{m}'' \rangle \equiv C_m \left\langle \frac{1}{\ell} \frac{1}{\ell} \frac{\nu}{\ell} \rho_1 \ell^3 \mid \text{DF} \right\rangle = C_m \rho_1 \langle \nu \mid \text{DF} \rangle, \quad (13)$$

which is constant because we take  $k$  and  $\Lambda$  as constant. Similarly, the dimensionless quantity  $\langle \dot{m}'' \rangle / (\rho_1 \langle \nu_d \rangle) = \langle \dot{m}'' \rangle / (C_{\nu_d} \rho_1 \langle \nu \mid \text{DF} \rangle) = C_m / C_{\nu_d}$ , a constant. The experiments of Sallam [11, pp. 53–54] show that this quantity increases with  $x$  from  $\mathcal{O}(10^{-2})$  to  $\mathcal{O}(1)$ . The inaccuracy could be due to the  $\langle \dot{m}'' \rangle$  model,  $\langle \nu_d \rangle$  model, or both.

For simplicity, we assume that  $\langle x_i \rangle = 0$  for the derivation of  $\langle x_b \rangle$ . Otherwise, a delay differential equation would be required to account for the delay between an eddy impacting the surface and droplet formation. After applying mass conservation for a particular realization of the jet to a differential element, we find that

$$\frac{d(\rho_1 A(x) \overline{U}_0)}{dx} = -P(x) \dot{m}'', \quad \text{or after rearrangement and averaging} \quad \frac{d\langle d_j \rangle}{dx} = -\frac{2\langle \dot{m}'' \rangle}{\rho_1 \overline{U}_0}, \quad (14)$$

where  $\overline{U}_0$  is the (constant) convection velocity, the jet is assumed to have a circular cross section,  $d_j(x)$  is the diameter of the jet at  $x$ ,  $A(x) = \pi d_j^2/4$  is the cross sectional area, and  $P(x) = \pi d_j$  is the perimeter. Consistent with how  $\langle x_b \rangle$  is measured, we define  $x_b$  with  $d_j(x_b) \equiv 0$ , so to first-order  $\langle d_j(\langle x_b \rangle) \rangle = 0$ . Solving equation 14 for  $\langle x_b \rangle$  with the  $\langle d_j(\langle x_b \rangle) \rangle = 0$  approximation using the  $\langle \dot{m}'' \rangle$  model (equation 13), we obtain

$$\frac{\langle x_b \rangle}{d_0} = \frac{\rho_1 \overline{U}_0}{2\langle \dot{m}'' \rangle} = \frac{\overline{U}_0}{2C_m \langle \nu \mid \text{DF} \rangle} = \frac{(\alpha - 2)}{2C_m(\alpha - 1)} \frac{\overline{U}_0}{v_{\text{min}}} = \frac{(\alpha - 2)\overline{U}_0}{2C_m(\alpha - 1)} \left( \frac{\rho_1}{\sigma \bar{\epsilon}_0} \right)^{1/5} = C_{x_b} \overline{Tu}_0^{-3/5} \left( \text{We}_{10} \frac{\Lambda_0}{d_0} \right)^{1/5}, \quad (15)$$

where we applied the result for a power law PDF,  $\langle v \mid DF \rangle = \langle v \mid v > v_{\min} \rangle = (\alpha - 1)v_{\min}/(\alpha - 2)$ , and also chose  $v_{\min} = v_{\sigma}$  (equation 4). We constructed a power law regression from the data we compiled [15, 28–30, 32] (185 points,  $R^2 = 0.9420$ , excluding  $\rho_1/\rho_g < 500$  data) valid for the second wind-induced regime with  $3.7 \cdot 10^3 < Re_{10} < 2.9 \cdot 10^5$ ,  $5.4\% < \overline{Tu}_0 < 12.7\%$ ,  $5.2 \cdot 10^2 < We_{10} < 1.2 \cdot 10^5$ , and  $5.7 \cdot 10^2 < \rho_1/\rho_g < 9.7 \cdot 10^3$ :

$$\frac{\langle x_b \rangle}{d_0} = 3.8911 \overline{Tu}_0^{-0.2685} We_{10}^{0.3273}. \quad (16)$$

The regression neglected  $Re_{10}$  and  $\rho_1/\rho_g$ . Including  $Re_{10}$  and  $\rho_1/\rho_g$ , their exponents would be 0.0207 and 0.0220 respectively, nearly zero, consistent with the theory. The signs of the  $\overline{Tu}_0$  and  $We_{10}$  exponents are correct, but the magnitudes are in error. The most likely cause of the error may be the model for  $\langle \dot{m}'' \rangle$ , as use of the  $\langle \dot{m}'' \rangle$  correlation from Sallam [11, p. 54],  $\langle \dot{m}'' \rangle \propto x/[\Lambda_0(We_{10}\Lambda_0/d_0)^{1/2}]$ , returns  $\langle x_b \rangle/d_0 \propto \overline{Tu}_0^{-3/10} We_{10}^{3/10}$ . We attempted to obtain the same  $\langle \dot{m}'' \rangle$  scaling using an exponential probability density function for  $t_b$  under the hypothesis that breakup takes time to become “fully developed”. We were able to obtain  $\langle \dot{m}'' \rangle \propto x$  to first-order (saturating far downstream), but the remainder of the scaling was incorrect. A better  $\langle \dot{m}'' \rangle$  model will be the subject of future work.

The regression was cross-validated with non-pipe  $\langle x_b \rangle$  data [17, 18]. This alternative data set has lower turbulence intensity ( $0.3\% < Tu_{c0} < 8.0\%$ ) than the pipe jets in our database ( $5.4\% < \overline{Tu}_0 < 12.7\%$ ). The fit between the regression and the alternative data was worse (79 points,  $R^2 = 0.5334$ ), but the error appeared random because its mean was roughly zero. The error possibly is due to variables not considered in the regression, e.g., the integral scale and the velocity profile. The error could also be due to Ervine et al. and McKeogh and Elsaywy measuring centerline  $Tu_{c0}$  rather than plane average  $\overline{Tu}_0$  as we have. The general agreement suggests that the regression may be valid for  $\overline{Tu}_0$  outside its calibration data and may be a useful model for non-pipe jets.

### Spray angle $\langle \theta \rangle$

Similar to previous works [3, 5, 12], we define the spray angle through  $\langle \tan \theta/2 \rangle \equiv \langle v_d/u_d \rangle$  (for  $x = \langle x_i \rangle$ ), so to first-order  $\tan \langle \theta \rangle/2 = \langle v_d \rangle/\langle u_d \rangle$ . As  $u_d = \overline{U}_0 + u$ , then  $\langle u_d \rangle \neq \overline{U}_0$  because there is an additional term with the correlation  $\langle uv \rangle$ . We assume this effect is negligible as we did for  $\langle x_i \rangle$ , so  $\langle u_d \rangle = \overline{U}_0$ . Then  $\tan \langle \theta \rangle/2 = \langle v_d \rangle/\overline{U}_0$ , so

$$\tan \left( \frac{\langle \theta \rangle}{2} \right) = C_{v_d} \frac{\overline{v}_0}{\overline{U}_0} \overline{Tu}_0^{-2/5} \left( We_{10} \frac{\Lambda_0}{d_0} \right)^{-1/5} = C_{v_d} \overline{Tu}_0^{3/5} \left( We_{10} \frac{\Lambda_0}{d_0} \right)^{-1/5}, \quad (17)$$

The power law regression of the data [5, 11, 25, 31, 33, 35] (20 points,  $R^2 = 0.7201$ ) is valid for  $6.7 \cdot 10^3 < Re_{10} < 7.3 \cdot 10^5$ ,  $4.4\% < \overline{Tu}_0 < 8.7\%$ ,  $3.9 \cdot 10^3 < We_{10} < 4.1 \cdot 10^5$ , and  $7.7 \cdot 10^2 < \rho_1/\rho_g < 8.8 \cdot 10^2$ :

$$\tan \left( \frac{\langle \theta \rangle}{2} \right) = 0.003113 \overline{Tu}_0^{-0.8730} We_{10}^{0.4294}. \quad (18)$$

We excluded  $Re_{10}$  due to confounding with  $\overline{Tu}_0$ . If included, the exponent of  $Re_{10}$  is small ( $-0.0426$ ), but inclusion of  $Re_{10}$  appreciably changes the exponent of  $\overline{Tu}_0$ . The model’s  $\overline{Tu}_0$  exponent is roughly correct, though the exponent’s uncertainty is large due to the small number of data points with strong  $\overline{Tu}_0$  variation. In our model  $\tan \langle \theta \rangle/2$  decreases with  $We_{10}$ , contrary to the regression. The only model we are aware of where  $\tan \langle \theta \rangle/2$  increases with  $We_{10}$  is that of Skrebkov [5, p. 145], who suggests that  $(\tan \langle \theta \rangle/2)^2 = \overline{Tu}_0^2 + 12C\rho_g/\rho_1 - 12/(DWe_{10})$  for high  $Re_{10}$ . The model of Huh et al. [12] has no  $We_{10}$  variation at all. The model of Tsyapko [7] is similar to Huh et al.’s, except for the addition of a term such that  $\tan \langle \theta \rangle/2$  is linear in  $Re_{10}$ . This is more correct, as both  $Re_{10}$  and  $We_{10}^{1/2}$  scale with  $\overline{U}_0$ , but ultimately  $Re_{10}$  is not  $We_{10}$ . In addition to previously discussed problems with the theory, these errors might be explained by the “velocity ratio” definition of spray angle ( $\langle \tan \theta/2 \rangle \equiv \langle v_d/u_d \rangle$ ) being incorrect.

### Summary and conclusions

While good agreement between current CDRSV theory and measurements was found for  $D_{32}$  and  $\langle x_i \rangle$ , the theory has not been validated for turbulent jet breakup in general, in part due to the failures of the theory with existing data, and also because  $\overline{Tu}_0$  varies little in existing data. Alternative modeling choices could improve accuracy. New experiments are needed to validate this class of theories, particularly experiments varying  $\overline{Tu}_0$ . Rough tubes are the easiest way to vary  $\overline{Tu}_0$  for a liquid jet, and are a prime opportunity for new experiments in our opinion.

### Acknowledgments

Prof. O. A. Ezekoye is thanked for suggestions and for focusing this work on the simpler fire hose case. Andrew Trettel of UCLA is thanked for discussions on single point velocity PDFs, among other topics related to this paper. University of Texas at Austin Interlibrary Services are also thanked for help obtaining many obscure papers.

## References

English translations of the papers by Natanzon [3], Tsyapko [6, 7], and Lebedev [8] are available from Ben Trettel.

- [1] Wu, P.-K. and Faeth, G. M. *Atom. and Sprays* 3(3) (1993): 265–289. DOI: 10.1615/AtomizSpr.v3.i3.20.
- [2] Lefebvre, A. H. and McDonell, V. G. *Atomization and Sprays*. 2nd ed. 2017. ISBN: 978-1-4987-3625-1.
- [3] Natanzon, V. Ya. *Dizelestroenie* (3) (1938): 3–10. OCLC: 145405221. LCCN: sv91018992.
- [4] Sitkei, G. NASA TT F-129. Oct. 1963. URL: <https://hdl.handle.net/2027/uiug.30112106740126>. Trans. of *Acta technica, Acad. Sci. Hung.* 25 (1-2 1959): 87–117. ISSN: 0001-7035.
- [5] Skrebkov, G. P. *Journal of Applied Mechanics and Technical Physics (FTD)* (3) (Feb. 1966): 142–151. URL: <http://www.dtic.mil/docs/citations/AD0635269>. Trans. of *Prik. mekh. i tekhn. fizika* (3) (May 1963): 79–83. ISSN: 0869-5032. URL: [http://www.sibran.ru/journals/issue.php?ID=160175&ARTICLE\\_ID=160248](http://www.sibran.ru/journals/issue.php?ID=160175&ARTICLE_ID=160248).
- [6] Tsyapko, N. F. *Voprosy gidravlicheskoj dobychi uglya: Trudy VNIIGidrouglya* 13 (1968): 12–18.
- [7] Tsyapko, N. F. *Voprosy gidravlicheskoj dobychi uglya: Trudy VNIIGidrouglya* 13 (1968): 18–19.
- [8] Lebedev, O. N. *Izv. Sib. otd. Akad. nauk SSSR, Ser. tekhn. nauk* 3(1) (1977): 40–44. ISSN: 0002-3434.
- [9] Wu, P.-K., Tseng, L.-K., and Faeth, G. M. *Atom. and Sprays* 2(3) (1992): 295–317. ISSN: 1044-5110. DOI: 10.1615/AtomizSpr.v2.i3.60.
- [10] Wu, P.-K. and Faeth, G. M. *Physics of Fluids* 7(11) (Nov. 1995): 2915–2917. ISSN: 1089-7666. DOI: 10.1063/1.868667.
- [11] Sallam, K. A. “Properties of Spray Formation by Turbulent Primary Breakup”. PhD Dissertation. Ann Arbor, MI: University of Michigan, 2002. URL: <https://search.proquest.com/docview/276490767>.
- [12] Huh, K. Y., Lee, E., and Koo, J. *Atom. and Sprays* 8(4) (1998): 453–469. DOI: 10.1615/AtomizSpr.v8.i4.60.
- [13] Kerstein, A. R., Movaghar, A., and Oevermann, M. *J. Fluid Mech.* 811(R5) (Jan. 2017). ISSN: 1044-5110. DOI: 10.1017/jfm.2016.806.
- [14] Trettel, B. ICLASS 2018. Chicago, IL, July 2018. Preprint DOI: 10.17605/OSF.IO/QSFP7.
- [15] Kusui, T. *Bulletin of JSME* 12(53) (1969): 1062–1071. ISSN: 0021-3764. DOI: 10.1299/jsme1958.12.1062.
- [16] Kim, S. “An Investigation of Heat and Mass Transport in Turbulent Liquid Jets”. PhD Dissertation. University of California, Los Angeles, 1983. OCLC: 11440592. NTRL: DE84011174.
- [17] Ervine, D. A., McKeogh, E., and Elsayy, E. M. *Proceedings of the Institution of Civil Engineers* 69(2) (June 1980): 425–445. ISSN: 1753-7789. DOI: 10.1680/iicep.1980.2545.
- [18] McKeogh, E. J. and Elsayy, E. M. *J. Hydraul. Div.* 106(10) (Oct. 1980): 1577–1593. ISSN: 0044-796X.
- [19] Mansour, A. and Chigier, N. *Physics of Fluids* 6(10) (Oct. 1994): 3380–3391. DOI: 10.1063/1.868396.
- [20] Wolf, D. H., Incropera, F. P., and Viskanta, R. *Experiments in Fluids* 18(6) (Apr. 1995): 397–408. ISSN: 0723-4864, 1432-1114. DOI: 10.1007/BF00208462.
- [21] Hinze, J. O. *Turbulence*. McGraw-Hill, 1975. ISBN: 978-0-07-029037-2.
- [22] Pope, S. B. *Turbulent Flows*. Cambridge University Press, 2000. ISBN: 978-0-521-59886-6.
- [23] Kolmogorov, A. N. *Selected Works*. Springer, 1991: 339–343. ISBN: 978-94-011-3030-1. DOI: 10.1007/978-94-011-3030-1\_50. Trans. of *Doklady AN SSSR* 66(5) (1949): 825–828. ISSN: 0002-3264.
- [24] Hinze, J. O. *AIChE Journal* 1(3) (Sept. 1955): 289–295. ISSN: 1547-5905. DOI: 10.1002/aic.690010303.
- [25] Wu, K.-J. “Atomizing Round Jets”. PhD Dissertation. Princeton University, 1983. OCLC: 82865393.
- [26] McCaslin, J. O. and Desjardins, O. ICLASS Americas 2015. Raleigh, NC, May 2015. URL: <http://www.ilass.org/2/database/Detail.aspx?AbstractID=1025>.
- [27] Wu, P.-K., Miranda, R. F., and Faeth, G. M. *Atom. and Sprays* 5(2) (1995): 175–196. ISSN: 1044-5110. DOI: 10.1615/AtomizSpr.v5.i2.40.
- [28] Chen, T.-F. and Davis, J. R. *J. Hydraul. Div.* 90(1) (Jan. 1964): 175–206. Erratum-ibid. 90(6) (Nov.): 273.
- [29] Grant, R. P. and Middleman, S. *AIChE Journal* 12(4) (July 1966): 669–678. ISSN: 1547-5905. DOI: 10.1002/aic.690120411.
- [30] Phinney, R. E. *AIChE Journal* 21(5) (Sept. 1975): 996–999. ISSN: 1547-5905. DOI: 10.1002/aic.690210523.
- [31] Hiroyasu, H., Shimizu, M., and Arai, M. *2nd ICLASS*. Madison, WI, June 1982: pp. 69–74. OCLC: 10261204.
- [32] Arai, M., Shimizu, M., and Hiroyasu, H. *3rd ICLASS*. Imperial College, London, UK, July 1985: IB/4/1–IB/4/10. OCLC: 18600142.
- [33] Ruff, G. A. “Structure and Mixing Properties of the Near-Injector Region of Nonevaporating Pressure-Atomized Sprays”. PhD Dissertation. Ann Arbor, MI: University of Michigan, 1990. URL: <https://search.proquest.com/docview/303861313>.
- [34] Miesse, C. C. *Ind. Eng. Chem.* 47(9) (Sept. 1955): 1690–1701. ISSN: 0019-7866. DOI: 10.1021/ie50549a013.
- [35] Reitz, R. D. “Atomization and Other Breakup Regimes of a Liquid Jet”. PhD Dissertation. Princeton University, 1978. URL: <https://search.proquest.com/docview/302918755>.
- [36] Hoyt, J. W. and Taylor, J. J. *J. Fluid Mech.* 83(1) (Nov. 1977): 119–127. DOI: 10.1017/S0022112077001074.